Proceedings of the 7th International Symposium on Cavitation
CAV2009
August 17-22, 2009, Ann Arbor, Michigan, USA

CAV2009 – Paper No. 112

EFFECTS OF SURFACE CHARACTERISTICS ON HYDROFOIL CAVITATION

Megan Williams
UC Berkeley
Berkeley, CA

Ellison Kawakami
University of Minnesota
Minneapolis, MN

Eduard Amromin
Mechmath, LLC
Prior Lake, MN

Roger Arndt
University of Minnesota
Minneapolis, MN

ABSTRACT

This was an exploratory research project aimed at capitalizing on our recent research experience with unsteady partially cavitating flows. Earlier work identified the significant and unexpected effect of surface properties and water quality on the dynamics of these flows. The aim of this study was to explore the possibility of using hydrophobic surfaces to control or minimize unwanted vibration and unstable operation in the partially cavitating regime. A candidate shape, denoted as the Cav2003 hydrofoil, was selected on the basis of theoretical analysis for a given range of contact angle. We manufactured three hydrofoils of identical cross section, but different surface characteristics. Three different surfaces were studied: anodized aluminium (hydrophilic), Teflon (hydrophobic), and highly polished stainless steel (hydrophobic). Contact angle was measured with a photographic technique developed by three of the undergraduates working on the project. Studies were made in both weak and strong water. Significant surface effects were found, but were unexpected in the sense that they did not correlate with measured contact angles.

INTRODUCTION

A variety of applications require operation in the cavitating regime. Associated with the deleterious effects of performance breakdown, noise, and vibration, there is a possibility of erosion. In many cases, unstable operation is caused by cavitation-induced flow instabilities. Cavitation is also known to produce air bubbles due to incondensable gas coming out of solution in low-pressure (supersaturated) regions of the flow. The production of bubbly flows in hydraulic equipment can have insidious effects on the stability of operation and on vibration.

A particularly important form of cavitation from a technical point of view is attached cavitation on the suction side of lifting surfaces. At typical angles of attack, this takes the form of a sheet, often terminated at the trailing edge by a highly dynamic form of cloud cavitation. Vortex cavitation is often observed in the cloud, which is caused by vorticity shed into the flow field. These cavitating microstructures are highly energetic and are responsible for significant levels of noise and erosion. The physics of these phenomena is easily studied with hydrofoils in a water tunnel (Kjeldsen et al, [1]).

This was an exploratory research project aimed at capitalizing on our recent research experience with unsteady partially cavitating flows over hydrofoils. Earlier work identified the significant and unexpected effect of surface properties and water quality on the dynamics of these flows. Previously it was thought that surface properties and water quality only affected cavitation inception physics. At the same time there has been significant interest in the use of hydrophobic surfaces for drag reduction. Hybrid drag reduction schemes involving a combination of microbubble injection coupled with the use of hydrophobic surfaces have also been proposed. The aim of this study was to explore the possibility of using hydrophobic surfaces to control or minimize unwanted vibration and unstable operation in the partially cavitating regime.

EXPERIMENTAL SET UP

A candidate shape, denoted as the Cav2003 hydrofoil, was selected on the basis of theoretical analysis for a given range of contact angle. We manufactured three hydrofoils of identical cross section, but different surface characteristics. Three different surfaces were studied: anodized aluminum (hydrophilic), Teflon (hydrophobic), and highly polished stainless steel (hydrophobic). Contact angle was measured with a photographic technique developed by three of the undergraduates working in the project. Contact angle measurements were made with drops and bubbles on candidate materials. The foils were tested in the SAFL high-speed water tunnel, which is equipped with a broad range flow measurement instrumentation. Water quality was varied by controlling the level of dissolved gas and through pressurization. (Arndt et al. [2])

ANALYSIS OF THE INFLUENCE OF SURFACE CHARACTERISTICS

It has been shown that an ideal fluid theory computation, utilizing an experimentally determined cavity detachment position, can provide a very satisfactory description of the cavity shape at given cavitation numbers (see Rowe and Blottiaux, [3], for example). Utilizing this concept, several authors have considered the connection between cavity detachment and laminar separation (Franc and Michel, [4]). As was discovered by Arakeri [5], a viscous separation zone is often located upstream of an attached cavity on a smooth body or hydrofoil. A meniscus in the cavity head acts as an obstacle causing this separation, as shown in Fig.1. Franc and Michel describe an iterative scheme whereby a potential flow model is used to compute the cavity shape based on an initial guess for the position of cavity detachment. A viscous-inviscid interaction concept permits the determination of the position of laminar separation and consequently the value for C_{ps} as shown in Figure 2. A similar approach can be taken to account for differences in contact angle as shown in the inset to Figure 2. Referring to Amromin [6] for more mathematical detail, we will consider the most basic effects in the vicinity of the cavity detachment from smooth surfaces.

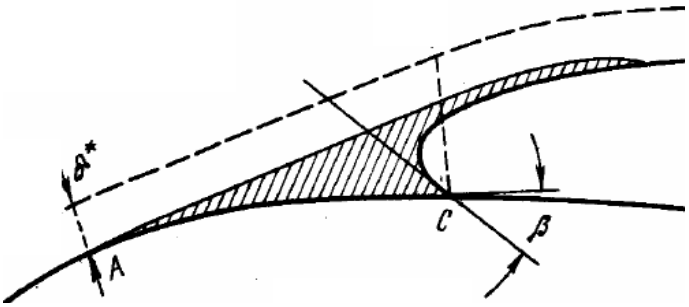

Figure 1: Sketch of cavity detachment zone. Striped area is the zone of laminar separation caused by the cavity: δ* is thickness displacement of the laminar boundary layer that separates from the wall and reattaches to the cavity surface. Adapted from Arakeri [5].

The surface wettability influences the size of this meniscus and its equilibrium point (cavity detachment point). The pressure distribution in the cavity detachment region is generally predetermined by the entire cavity volume (and its length), whereas the surface material-dependent difference in the cavity nose curvature makes a secondary effect on Cp. Because this meniscus-nose is submerged within a laminar separation zone of practically constant pressure we can write

$$\sigma = -C_{ps} + 2cWe / R \qquad (1)$$

Here R is curvature radius of the cavity surface, We is Weber number based on chord length, c. One can see that for a fixed pair {σ, We}, R will be also fixed. On the other hand, R can be represented through the local cavity thickness b(x) as R=b/(1+cosβ). Therefore the b value in the detachment point varies inversely with β down to 0 inherent to hydrophobic surfaces and the cavity detachment moves downstream to the thicker cavity part, as in Fig.2. Secondly, the β effect is smaller for contours with greater Cp gradients (as in the experiments with a sphere by Leder and Ceccio [7], relative to experiments with an oblong ellipsoid described by Amromin and Ivanov, [8]).

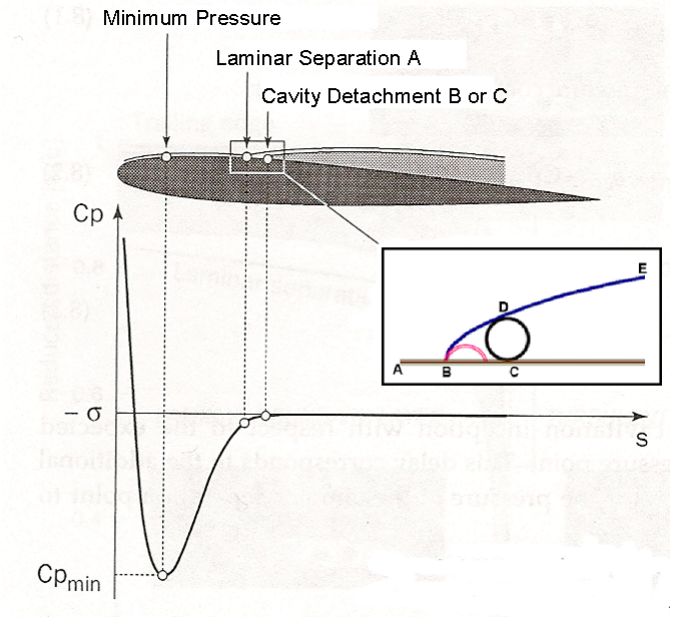

Figure 2: Illustration of the viscous-inviscid iteration concept. As shown, the pressure distribution upstream of the cavity corresponds to pressure less than vapor pressure (tension). A is the point of laminar boundary layer separation from the surface[1]. The inset illustrates the comparison of the cavity detachment regions for hydrophilic and hydrophobic surfaces. The cavity boundary is the curve BDE for a Teflon surface with a contact angle β = π/2 and the curve CDE for an aluminum surface with an assumed contact angle β=0. (Adapted from Franc and Michel, [4]).

[1] This model is appropriate for situations where there is a dearth of nuclei, i.e. "strong water"

The geometrical view of Fig.2 can be supplemented by a formal consideration. Let us rewrite Eq.(1) for the meniscus as

$$\frac{\sigma + C_{ps}}{2We} = c\frac{d^2y/dx^2}{\left[1+(dy/dx)^2\right]^{3/2}} \qquad (2)$$

This second-order ordinary differential equation must be integrated with the "matching" boundary condition on the cavity y(E)=Ycavity (E) and with two β-dependent boundary conditions on y and dy/dx at a selected cavity detachment point. Such integration is possible only with fitting of the Weber number. Thus, the numerical algorithm is a two-task semi-inverse algorithm here: First, for the selected the cavity detachment and end, the Cp distribution and σ value must be found. Second, for the selected β and Reynolds number, the Weber number (and, correspondingly, the hydrofoil/body size) must be found.

APPROACH TO COMPUTATION OF CAVITATION INCEPTION NUMBER

Cavitation inception number is defined here as the maximum cavitation number corresponding to a steady attached cavity in strong water. Weak water will probably result in bubble cavitation at the minimum pressure point negating the assumptions in the proposed model. For strong water, the cavity pressure is close enough to the vapor pressure.

It also important to note that the maximum of σ does not corresponds to the minimum mathematically possible cavity length because of the capillarity effect. As shown in Figs.3 and 4, there is usually a range of σ with two solutions, but only the solution with larger cavities is physically attainable (possibly, in the accordance with Dirichlet principle on the minimum of potential energy in a mechanical system). Further, for cavitation inception in regions of a substantial pressure gradient (like for hydrofoil in Fig.4), the cavity length corresponding to σ_I is much smaller and may be too small for visual determination.

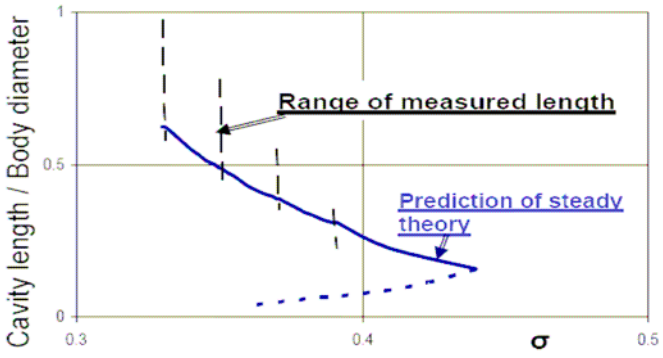

Figure 3: Comparison of observed (by Ceccio and Brennen, [9]) and computed (by Amromin, [6]) cavity lengths on the ITTC axisymmetric body (0.05m diameter).

Further, the computed values of cavitation number are mainly smaller than the experimental values and, besides the drawbacks of the theoretical cavity concept, it may occur due to at east two errors: First, the wall effect may be computationally underestimated. Second, the water tunnel air content may be high enough to cause an overestimation of cavitation number in the experiments. The second error looks to be dominant for bubbly cavitation.

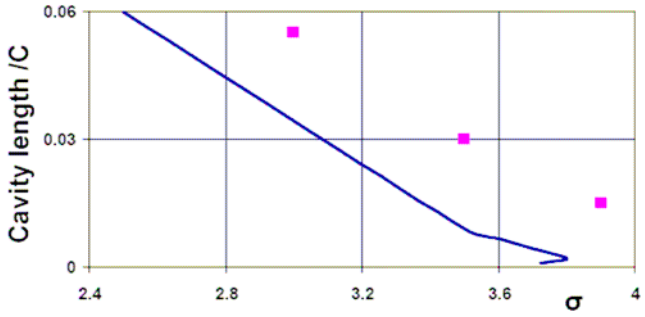

Figure 4: Comparison of computed and observed (after Amromin et al, [10]) cavity length on NACA-16009 hydrofoil with C=0.1m at 5 degree angle of attach in a narrow water tunnel.

As noted, there is an issue of determining the difference of the real cavitation number and the theoretical cavitation number calculated with the assumption that the cavity pressure equals the vapor pressure. The sum $s = \sigma_I + Cp$ for the bubbly cavitation at zero angle of attack for the symmetrical hydrofoil can be considered as a first-approach correction that must be deducted from the vapor cavitation number to determine the real cavitation number (though an exact correction should be greater).

Another issue is in determination of hydrofoil lift dependency on its angle of attack.

RESULTS

Contact angle measurements were made with drops and bubbles on candidate materials as illustrated in Figure 5. Our contact angle measurements indicated that there was very little difference for the surfaces studied. However, the polished stainless steel surface had remarkably different cavitation characteristics. Unexpectedly, the Teflon and anodized aluminum surfaces were similar in their cavitation characteristics. Based on the measured range of contact angles, we predicted the change in cavity length and estimated the change in lift dynamics on the basis of our previous experiments and with the help of our numerical model. We found that the model had to be revised to fit the observations.

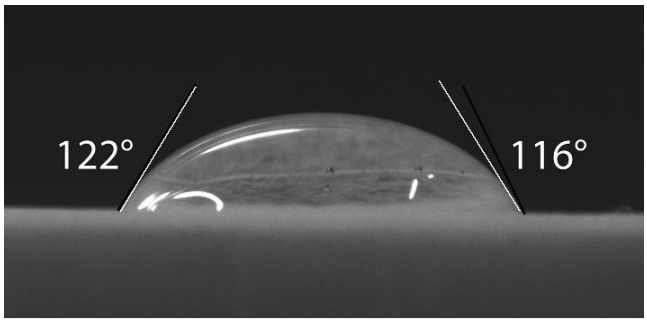

Figure 5. Contact of a drop on a relatively hydrophilic surface. Angle shown = $\pi - \phi$

An extensive set of high-speed video observations was also made. Our first discovery was that sheet cloud cavitation could not be detected at the same angles of attack that we used in our studies of a NACA 0015 foil. In fact, sheet cloud cavitation was limited to a very narrow range of angle of attack. This was actually predicted in a numerical study performed four years earlier (Qin, [11]).

An angle of attack of four degrees was selected for detailed study. Measurements were made in both weak and strong water so that six data sets were available for detailed analysis. One of the unexpected results was the significantly different dynamics of cavitation was found on the polished stainless steel hydrofoil. Depending on the cavitation number, the fully wetted time observed during a cavitation cycle was observed to be as high as 50%. Variation in water quality as well as surface characteristics also produced significantly different levels of unsteady lift.

One of the motivations in believing that surface characteristics would play a role in sheet cloud cavitation is the observation that even under intense oscillatory flow a hydrofoil can become fully wetted for period during a fraction of each oscillation period. This is illustrated in Figure 6 (Kawakami et al, [12]. Note the significant increase in dwell time for stainless steel. This was one of the factors considered in the current study as shown in Figure 7. Note that any fully wetted period occurred over a narrower range of $\sigma/2\alpha$ and the effect was much less noticeable. The reason for the differences is not fully understood. We were not able to observe any fully wetted phenomena with the stainless steel Cav 2003 foil at 6° or 8° as was the case of for observations on a NACA 0015 foil shown in Figure 6. Fully wetted phenomena were only detected at relatively low angles of attack. Hence the data in Figure 7 correspond to an angle of attack of 4 degrees. A sequence of stages in the oscillation cycle is shown in Figure 8.

Cavitation inception studies also provided further insight. As expected, the inception physics change drastically at an angle of attack between 2 and 3 degrees. This is due to the dramatic shift in the minimum pressure position from mid chord to the leading edge as shown in Figure 9. A significant finding was that for angle of attack less than 3 degrees, there is no measurable effect of either the surface characteristics or water quality. There is, however, a significant effect of both surface characteristics and water quality at higher angles of

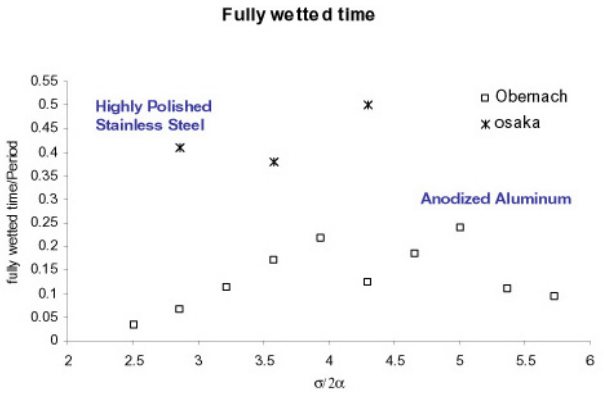

Figure 6. Fully wetted time on a NACA 0015 hydrofoil (Kawakami et al, 2008)

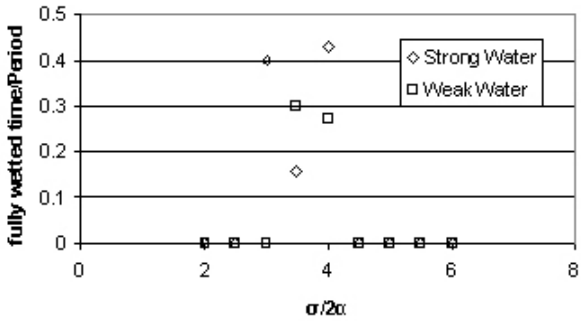

Figure 7. Fully wetted time on a stainless steel Cav 2003 hydrofoil at 4° angle of attack

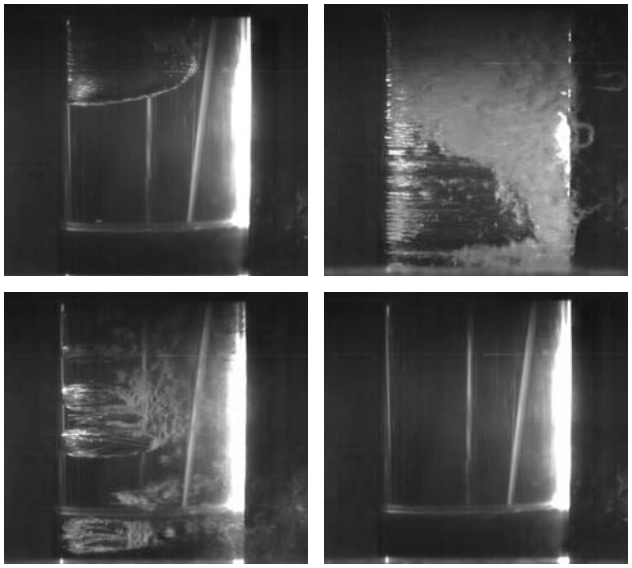

Figure 8. Stainless steel in weak water. $\alpha = 4°$, $\sigma/2\alpha = 4$. View of cavitation at different stages in the oscillation cycle: Top Left: t = 0.142 period Top Right: t = 0.585 period Lower Left: t = 0.803 period Lower Right: Fully Wetted One period was equivalent to a time of 0.06 seconds. Flow is from left to right

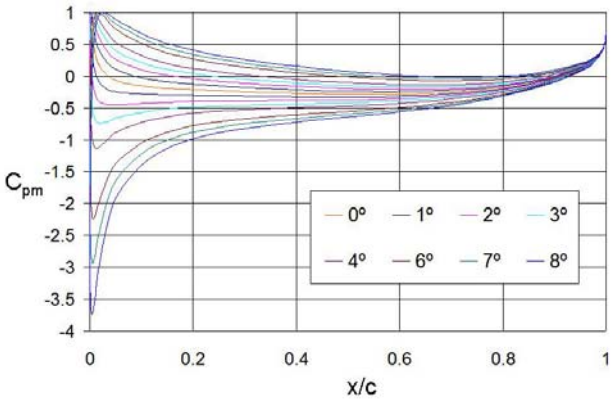

Figure 9. Pressure coefficient, Cav 2003

attack. As shown in Figure 10, where the data deviate in a consistent manner from $-C_{pm}$ with increasing angle of attack. There is also a measurable effect of the type of surface and water quality. Also shown in Figure 10 is a comparison with the data of Coutier-Delgosha et al. [13] who also performed inception measurements with the Cav 2003 hydrofoil. The agreement is very good, lending support the observations shown here.

A full explanation for the noted effects of both water quality and surface characteristics is not at hand. However, as shown in Figure 11, the trend is qualitatively predicted by Amromin [6]. His results are calculations of the difference between the minimum pressure coefficient and σ for hydrophilic and hydrophobic surfaces. However, his theory, which is based on the model shown in Figure 5, is for sheet cavitation whereas inception was observed to be mainly patch cavitation. In addition, the predicted difference between hydrophilic and hydrophobic surfaces was not noted in the experiments. Hence a complete explanation of our results is not at hand.

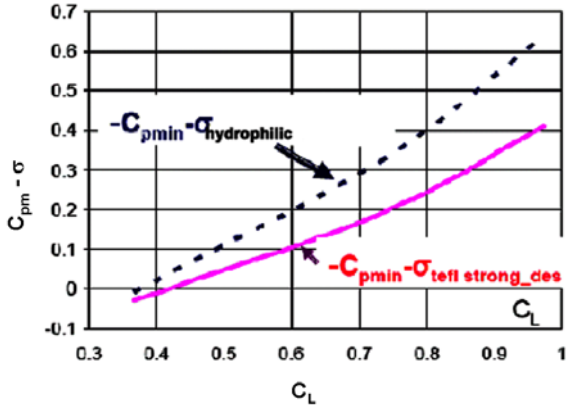

Figure 11 Calculation of $-C_{pm} - \sigma$ by Amromin [6]

CONCLUSION

The results of this will research are mixed. We found that surface characteristics have a significant effect on cavitation induced vibration and unsteadiness, but we were not able to correlate the differences with our contact angle measurements. We are continuing to purse this research, since it shows great potential for elucidating some new cavitation physics

ACKNOWLEDGMENTS

This work was supported by NSF under the SGER program. Dr. William Schultz was the contract monitor. Mr. Eric Axdahl initiated the contact angle measurement technique and Dr. William Hambleton assisted with the preliminary experimental setup.

NOMENCLATURE

c = chord length
C_L = lift coefficeint
C_p = pressure coefficient
f = frequency

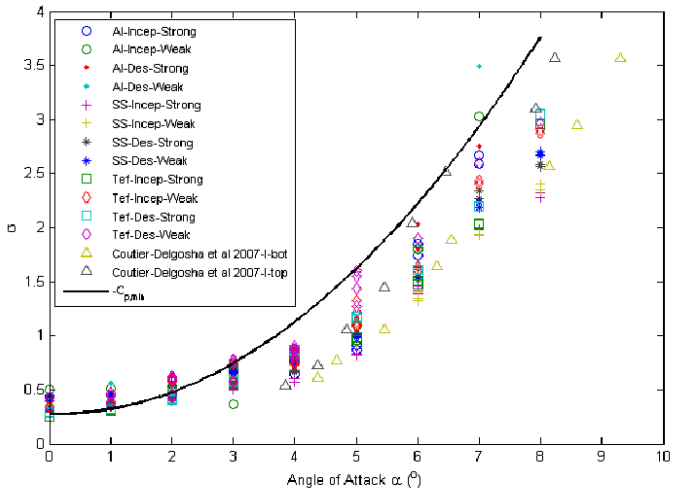

Type of Cavitation

0 deg - bubble
1 deg - bubble
2 deg - bubble
3 deg - bubble
4 deg - bubble/patch
5 deg - patch
6 deg - patch
7 deg - patch
8 deg - patch

Figure 10 Inception Data for the Cav 2003 hydrofoil

R = radius of curvature
U = free stream velocity
p_o = free stream pressure
p_v = vapor pressure
α = angle of attack
ϕ = contact angle
σ = cavitation number

REFERENCES

1. Kjeldsen M, Arndt REA, Effertz M (2000) Spectral characteristics of sheet/cloud cavitation. *J Fluids Eng* 122:481-487
2. Arndt, R.E.A., Kawakami, D. and Wosnik, M. "Measurements In Cavitating Flows" *Handbook of Fluid Mechanics Measurements,* Springer-Verlag, Berlin, December 2007
3. Rowe, A. and Blottiaux, O. 1993 *Aspects of Modeling Partially Cavitating Flows*. J. Ship Research, v37, pp39-50
4. Franc, J-P, and Michel J-M, 2004 *Fundamentals of Cavitation* Kluwer Academic Publishers
5. Arakeri, V.H. 1975 "Viscous effects on the position of cavitation separation from smooth bodies", J. Fluid Mech., **68**,pp779-799
6. Amromin,E.L. 2007 "Determination of cavity detachment for sheet cavitation" *J. Fluids Eng,* v129,pp1105-1111
7. Leder, A.T. and Ceccio, S.L. 1998 "Examination of the flow near the leading edge of attached cavitation. Part 1: Detachment of two-dimensional and axisymmetric cavities" *J. Fluid Mech*., v376, pp61-90
8. Amromin, EL and Ivanov, AN, 1982 "Determination of Cavity Separation Points on Body in Viscous Capillary Fluid". PHYSICS-DOKLADY, , v.262, N4
9. Ceccio, S.L. and Brennen, C.E. 1992 "Dynamics of sheet cavities on bodies of revolution", J. Fluids Eng., **114**, pp 93-99
10. Amromin, E.L., Vaciliev, A.V. and Briancon-Marjollet, L. 1994 "Sheet Cavitation: Comparison between Measured and Calculated Length". *Intern. Shipbuilding. Conf.* v.B, St.-Petersburg
11. Qin Q (2004) Numerical Modeling of Natural and Ventilated Cavitating Flows, *PhD Thesis*, University of Minnesota
12. Kawakami, DT, Fujii, A, Tsujimoto, Y and Arndt, REA (2008) An assessment of the influence of environmental factors on cavitation instabilities, *J. of Fluids Eng* **130**, 031303-1-8
13. Coutier-Delgosha, O, Deniset, F, Astolfi, JA and Leroux, J-B, 2007, "Numerical Prediction of Cavitating Flow on a Two-Dimensional Symmetrical Hydrofoil and Comparison to Experiments" *Journal of Fluids Engineering,* **129,** March